Ann Dermatol. 2025 Jun;37(3):152-161
https://doi.org/10.5021/ad.25.001
pISSN 1013-9087·eISSN 2005-3894

ANNALS of DERMATOLOGY

Original Article

Check for updates

Electrical Stimulation Using a Low-Frequency and Low-Intensity Alternating Current Modulates Type I Procollagen Production and MMP-1 Expression in Dermal Fibroblasts

Bo Mi Kang [1,2], **Jung Min Ahn** [1,2], **Jieun Kim** [3], **Kyungho Paik** [1,2], **Bo Ri Kim** [1,2], **Dong Hun Lee** [3], **Sang Woong Youn** [1,2], **Keun-Yong Eom** [4], **Chong Won Choi** [1,2]

[1]Department of Dermatology, Seoul National University Bundang Hospital, Seongnam, Korea
[2]Department of Dermatology, Seoul National University College of Medicine, Seoul, Korea
[3]Institute of Human-Environment Interface Biology, Medical Research Center, Seoul National University, Seoul, Korea
[4]Department of Radiation Oncology, Seoul National University Bundang Hospital, Seongnam, Korea

OPEN ACCESS

Received: Jan 1, 2025
Revised: Mar 4, 2025
Accepted: Mar 5, 2025
Published online: Mar 19, 2025

Corresponding Authors:
Keun-Yong Eom
Department of Radiation Oncology, Seoul National University Bundang Hospital, Seoul National University College of Medicine, 82 Gumi-ro, 173beon-gil, Seongnam 13620, Korea.
Email: 978sarang@hanmail.net

Chong Won Choi
Department of Dermatology, Seoul National University Bundang Hospital, Seoul National University College of Medicine, 82 Gumi-ro, 173beon-gil, Seongnam 13620, Korea.
Email: cwonchoi@snu.ac.kr

ABSTRACT

Background: Despite various therapeutic modalities for keloids have been introduced; however, their therapeutic effects are limited. Therefore, the development of a new approach for inhibiting collagen production by scar fibroblasts is needed.
Objective: To investigate the effect of electrical stimulation using a low-frequency and low-intensity alternating current on collagen and MMP-1 levels in human dermal fibroblasts.
Methods: Low-frequency (20 kHz) and low-intensity (1 V/cm) electrical stimulations were applied to primary dermal fibroblasts. The production of type I procollagen and expression of matrix metalloproteinase-1 were evaluated. Transcriptomic analyses were conducted to explore the possible modes of action of electrical stimulation.
Results: Electrical stimulation effectively suppressed type I procollagen production and increased MMP-1 expression. In addition, transcriptomic analyses revealed that electrical stimulation altered the gene expression associated with membrane permeability and the structure of cellular membranes. Validation using real-time polymerase chain reaction revealed that electrical stimulation significantly altered the expression of mechanosensitive ion channels (*PIEZO2*) and membrane-bound protein organizing caveolae (*CAVIN2*).
Conclusion: Electrical stimulation using low-frequency and low-intensity alternating currents effectively modulates extracellular matrix homeostasis by altering the cellular membrane structure and function. Our findings suggest a promising therapeutic approach for the management of keloids and hypertrophic scars.

Keywords: Electrical stimulation; Extracellular matrix; Fibroblast; Matrix metalloproteinase-1; Procollagen

INTRODUCTION

Numerous studies have been performed on the effects of electrical stimulation on human cells or tissues to promote cellular function. In the skin, some studies have focused on improving the proliferation of fibroblasts and keratinocytes, promoting extracellular matrix (ECM) production of fibroblasts, and remodeling collagen fibrils to promote wound healing[1,2]. Electrical stimulation has beneficial effects in the treatment of diabetic foot ulcers[3]. Other studies have also reported the efficacy of electrical stimulation for management of various types of chronic skin ulcers[4,5]. In addition to promoting cellular function via electrical stimulation, attempts to use electrical stimulation for cancer treatment have been made. Using an alternating current (AC) of moderate frequency (100–300 kHz) and low-intensity (1–3 V/cm), electrical stimulation demonstrated an inhibitory effect on cell growth in glioblastoma, lung cancer, and mesothelioma[6]. Based on this inhibitory effect of electrical stimulation, the Food and Drug Administration approved the use of electrical stimulation as a noninvasive physical therapy for glioblastoma[7]. Although the inhibition of cell division by modulating cell and nuclear membrane permeability was suggested as the mechanism of action, the mechanism of electrical stimulation with intermediate frequency and low-intensity AC in malignant tumors remains unclear[6,7].

Hypertrophic scars and keloids are fibroproliferative disorders of the skin caused by a dysregulated wound-healing process. Previous studies have found that fibroblasts in hypertrophic scars and keloids produce increased levels of collagen, which is responsible for the fibrotic tissue in the dermis[8,9]. To date, various treatment modalities, including intralesional triamcinolone injection, pulsed dye laser, fractional laser, and cryotherapy, have been introduced for hypertrophic scars and keloids; however, their therapeutic effects are limited. Therefore, a new approach for inhibiting collagen production by scar fibroblasts should be developed.

As for the use of electrical stimulation for hypertrophic scar and keloid skin, there were few *in vivo* studies. Previously, Perry et al.[10] reported that non-invasive electrical stimulation significantly reduced scar scores as well as the symptoms of scar. Moreover, a recent *in vitro* study found a decreased collagen production in fibroblasts intermittently treated with an AC current of 448 kHz[11]. In this study, we studied the effects of electrical stimulation using a low-frequency and low-intensity AC on collagen and MMP-1 production in human dermal fibroblasts.

MATERIALS AND METHODS

Cell culture

Primary human skin fibroblasts were cultured in Dulbecco's modified Eagle medium (Welgene, Daegu, Korea) containing 10% fetal bovine serum (Gibco, Rockville, MD, USA) and 1% penicillin (Gibco) at 37°C in a humidified incubator with 5% CO_2.

Electrical stimulation of human dermal fibroblasts

To apply electrical stimulation to the cells, we designed an electrode and an electrical stimulation system, as shown in **Fig. 1A**. Stainless steel was used for the electrodes to prevent chemical reactions with the cell culture fluid. The electrodes were spaced 1 cm apart, and both ends were monitored using an oscilloscope (SDS1204X-E; Siglent Technologies, Solon, OH, USA). A Kool-ertron DDS signal generator (Karson Technology, Hong Kong) was used to generate the required amplitude and frequency and was connected to an amplifier and power supply to maintain a constant current and voltage. The voltage was adjusted to deliver a 1 V, 20 kHz sine wave across the electrodes. The electrode was positioned immediately above the cell surface to ensure a close contact with the cell.

Quantitative reverse transcription polymerase chain reaction (RT-PCR)

Isolation of total RNA from primary human dermal fibroblasts was performed using TRIzol reagent (Invitrogen, MA, USA) according to the manufacturer's instructions. Subsequently, 3.0 μg of extracted total RNA was used for cDNA synthesis using the First Strand cDNA Synthesis Kit (Thermo Fisher Scientific, Waltham, MA, USA). The evaluation of expression level of mRNA was performed using 7500 Real Time PCR system (Applied Biosystems, Foster City, CA, USA) and AccuPower® 2X GreenStar™ qPCR Master Mix (Bioneer, Daejeon, Korea). The $2^{-\Delta\Delta Ct}$ method was used to determine the relative changes in the expression of the target genes normalized to that of GAPDH.

Western blotting

After electrical stimulation, human dermal fibroblast-conditioned media and total cell lysates were harvested. Equal aliquots of conditioned culture media were separated using 8% sodium dodecyl sulfate polyacrylamide gel, and the transferred onto polyvinylidene fluoride membranes. After blocking with 5% skim milk (Difco™ Skim Milk; 232100; BD, Franklin Lakes, NJ, USA) in 1× phosphor-buffered with 0.1% Tween 20 and probed with monoclonal anti-procollagen type I amino-terminal extension peptide (SP1.D8) (Developmental Studies, Hybridoma Bank, Iowa City, IA, USA), anti-MMP1 (ab137332; Abcam, MA, USA; 1/1,000 dilution), and anti-β-actin (13E5; Cell Signaling Technology, Danvers, MA, USA; 1:1,000) antibodies. Horseradish peroxidase-conjugated goat anti-rabbit antibody was used as the secondary antibody (32460; Invitrogen; 1:10,000).

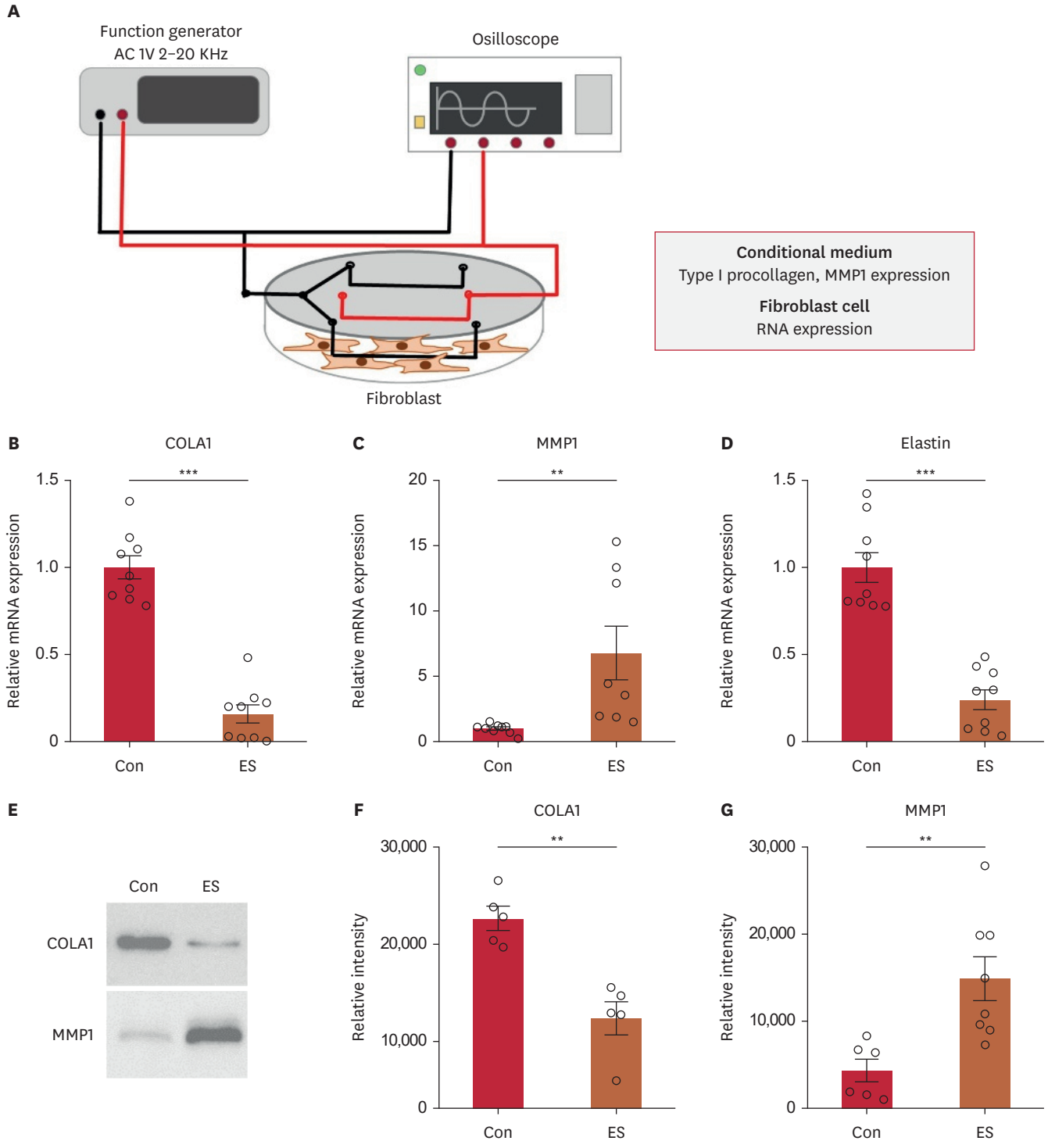

Fig. 1. Electrical stimulation modulated the synthesis of ECM protein. (A) Diagram of apparatus for electrical stimulation. (B-D) Real-time PCR analysis of ECM in primary dermal fibroblasts after electrical stimulation. (E-G) Western blot analysis of type I procollagen and matrix metalloproteinase-1 using culture media after electrical stimulation.
ECM: extracellular matrix.
$^{**}p<0.01$, $^{***}p<0.001$.

https://doi.org/10.5021/ad.25.001

Gene silencing via siRNA transfection

Primary human skin fibroblasts were seeded and transfected with the negative control siRNA or siRNA specific for *PIEZO2* and *CAVIN2* using RNAiMAX (13778; Invitrogen). The control scrambled siRNA was obtained from Bioneer. The siRNA sequences used were as follows:

CAVIN2, forward 5′-GUAGAAUGUCUCCAAGAUU-3′ and reverse 5′-AAUCUUGGAGACAUUCUAC-3; *PIEZO2,* forward 5′-CUCUUGCUCAUUCCUCUGU-3′ and reverse 5′-ACAGAGGAAUGAGCAAGAAGAG-3′.

The culture medium was changed 6 hours after transfection, and the cells were incubated at 37°C in a CO_2 incubator. After 24 hours, human dermal fibroblasts were lysed using TRIzol reagent (Invitrogen) according to the manufacture's instructions.

RNA sequencing (RNAseq) analysis

After electrical stimulation, human dermal fibroblasts were placed in RNAlater solution (Thermo Fisher Scientific). RNA extraction, sequencing, statistical analysis were performed by Macrogen Inc. (Seoul, Korea).

Statistical analysis

GraphPad Prism (version 8.0; GraphPad Software Inc., La Jolla, CA, USA) was used for statistical analyses. Mann–Whitney tests and one-way analysis of variance followed by Tukey's post hoc test was used for comparing the differences between two groups and among multiple groups, respectively. Statistical significance was set at p-value <0.05. Individual values (p<0.001, p<0.01, and p<0.05) are shown.

Ethics statement

This study was conducted in accordance with the principles of the Declaration of Helsinki. All experiments were approved by the Institutional Review Board (IRB) of Seoul National University Hospital (IRB No: H-1101-116-353).

RESULTS

Electrical stimulation decreased type I procollagen production and increased MMP-1 expression in primary human dermal fibroblasts

First, we investigated the effects of electrical stimulation on the synthesis of type I procollagen and MMP-1 in dermal fibroblasts. After 12 hours of starvation, the cells were treated with electrical stimulation using low-frequency and low-intensity AC (20 kHz, 1 V/cm). Electrical stimulation for 24 hours significantly decreased the mRNA levels of type I procollagen and elastin and increased that of MMP-1 in primary human dermal fibroblasts (**Fig. 1B-D**). Moreover, western blot analysis using culture media demonstrated a significant change after electrical stimulation; levels of type I procollagen in the culture medium significantly decreased, while electrical stimulation increased MMP-1 production (**Fig. 1E-G**). Collectively, these findings strongly suggested that electrical stimulation effectively suppresses type I procollagen production, while upregulates MMP-1 expression in dermal fibroblasts. Cell viability measured by Annexin V and PI staining was not affected by electrical stimulation of primary human dermal fibroblasts (**Supplementary Fig. 1**).

Transcriptomic analyses suggest the mechanism of modulation of type I procollagen production and MMP-1 expression in dermal fibroblasts

Next, we studied the plausible mode of action by which electrical stimulation modulates type I procollagen production and MMP-1 expression in dermal fibroblasts. Our mRNA transcriptomic analyses using RNAseq showed that electrical stimulation using low-frequency and low-intensity AC produced 464 DEGs (both |Fold change|≥2; p<0.05; **Fig. 2A and B**). Based on Kyoto Encyclopedia of Genes and Genomes (KEGG) analysis, electrical stimulation of dermal fibroblasts affected genes related to the collagen-containing ECM, monoatomic ion channel complex, and apical plasma membrane (**Fig. 2C and D**). Other signaling pathways of interest that were affected by electrical stimulation were transmembrane transporter complexes, membrane rafts, and voltage-gated potassium channel complexes. In addition, we performed Gene Ontology (GO) functional analyses to identify the potential targets of electrical stimulation in primary human fibroblasts. Electrical stimulation altered the collagen-containing ECM in the cellular components (**Fig. 2E and F**). In addition, the results suggested that various ion channel complexes and fibroblast membranes, including the plasma membrane, were affected by electrical stimulation. The 40 most significant DEGs after electrical stimulation of primary human fibroblasts are summarized in **Table 1**. These results suggested that the modulation of type I procollagen production and MMP-1 expression in dermal fibroblasts is associated with changes in the function of the membrane and its ion channels induced by electrical stimulation.

Validation of DEGs using quantitative RT-PCR

Based on our RNA-seq results, we hypothesized that electrical current alters the function of cell membranes and various ion channels present in dermal fibroblasts, thereby influencing type I procollagen production and MMP-1 expression. With this hypothesis, we examined the components of cell membranes and ion channels involved in the development of hypertrophic scars and keloids using existing literature reports and compared these findings with our RNA-seq results. Among the various genes, we selected two genes, *PIEZO2* and *CAVIN2,* for qRT-PCR analysis to

Fig. 2. Transcriptomic analyses. (A) Cluster analysis of DEGs. The color of the heat map indicates relative gene expression: brighter yellow and deeper blue indicate higher and lower gene expression, respectively. (B) Comparison of up- and downregulated genes (yellow, upregulated; blue, downregulated). (C) KEGG enrichment analysis of upregulated DEGs. (D) Smear plot of up- and downregulated genes. (E) GO functional analysis of cellular components. (F) Scatter plot of up- and downregulated genes.
KEGG: Kyoto Encyclopedia of Genes and Genomes, GO: Gene Ontology.

https://doi.org/10.5021/ad.25.001

Table 1. Top 40 up- and downregulated genes in fibroblasts after electrical stimulation

Gene_ID	Gene name	Gene description	Log2 FC	*p*-value	Adjusted *p*-value
Top down regulated genes					
142910	LIPJ	Lipase family member J	−23.024334	0.001782286	0.706148979
9865	TRIL	TLR4 interactor with leucine rich repeats	−22.374811	6.45E-5	0.096353188
267004	PGBD3	PiggyBac transposable element derived 3	−22.143039	0.002116575	0.775305577
4072	EPCAM	Epithelial cell adhesion molecule	−17.166666	0.000467231	0.335956629
115572	TENT5B	Terminal nucleotidyltransferase 5B	−14.914450	0.000345488	0.279471121
55799	CACNA2D3	Calcium voltage-gated channel auxiliary subunit alpha2delta 3	−14.518743	0.002516721	0.790569057
4129	MAOB	Monoamine oxidase B	−13.450035	0.000430265	0.321275593
4232	MEST	Mesoderm specific transcript	−12.522595	0.000210974	0.204792663
100499483	CCDC180	Coiled-coil domain containing 180	−12.400525	0.000862769	0.495053091
338811	TAFA2	TAFA chemokine like family member 2	−11.803153	0.001601365	0.647685392
100631383	FAM47E-STBD1	FAM47E-STBD1 readthrough	−11.491570	0.000198529	0.20285525
51384	WNT16	Wnt family member 16	−11.457720	0.003112808	0.934306823
101927655	ZASP	ZO-2 associated speckle protein	−11.253543	0.007434817	1
2255	FGF10	Fibroblast growth factor 10	−10.837236	0.000263326	0.243031891
1141	CHRNB2	Cholinergic receptor nicotinic beta 2 subunit	−10.506228	0.004547753	1
8436	CAVIN2	Caveolae associated protein 2	−10.423505	0.000492385	0.34139891
100526693	ARPC4-TTLL3	ARPC4-TTLL3 readthrough	−10.400079	0.00032277	0.272446084
124	ADH1A	Alcohol dehydrogenase 1A (class I), alpha polypeptide	−9.387715	0.015150304	1
100133941	CD24	CD24 molecule	−9.237573	0.007826126	1
8743	TNFSF10	TNF superfamily member 10	−9.079592	0.000606692	0.392610455
643338	C15orf62	Chromosome 15 open reading frame 62	−8.919707	0.003998158	1
6357	CCL13	C-C motif chemokine ligand 13	−8.679708	0.006319303	1
11170	FAM107A	Family with sequence similarity 107 member A	−8.675357	0.002436393	0.790569057
29841	GRHL1	Grainyhead like transcription factor 1	−8.496681	0.001185659	0.590214826
4675	NAP1L3	Nucleosome assembly protein 1 like 3	−8.365846	0.001550925	0.640630951
125	ADH1B	Alcohol dehydrogenase 1B (class I), beta polypeptide	−8.296212	0.000889987	0.495053091
64919	BCL11B	BAF chromatin remodeling complex subunit BCL11B	−8.286082	0.012140675	1
7730	ZNF177	Zinc finger protein 177	−8.187467	0.003181985	0.935985829
284040	CDRT4	CMT1A duplicated region transcript 4	−8.163663	0.000892493	0.495053091
79656	BEND5	BEN domain containing 5	−8.110509	0.00472768	1
6356	CCL11	C-C motif chemokine ligand 11	−8.056228	0.001422409	0.615661579
7472	WNT2	Wnt family member 2	−8.017266	0.00084909	0.495053091
653567	TMEM236	Transmembrane protein 236	−7.988343	0.027322057	1
54821	ERCC6L	ERCC excision repair 6 like, spindle assembly checkpoint helicase	−7.521886	0.033664757	1
389125	MUSTN1	Musculoskeletal, embryonic nuclear protein 1	−7.521886	0.033664757	1
338382	RAB7B	RAB7B, member RAS oncogene family	−7.405789	0.001300185	0.615661579
3627	CXCL10	C-X-C motif chemokine ligand 10	−7.389110	0.00139584	0.615661579
150590	C2orf15	Chromosome 2 open reading frame 15	−7.334591	0.019434951	1
63895	PIEZO2	Piezo type mechanosensitive ion channel component 2	−7.250286	0.006383312	1
Top up regulated genes					
341405	ANKRD33	Ankyrin repeat domain 33	24.735333	4.15E-5	0.094067798
4071	TM4SF1	Transmembrane 4 L six family member 1	18.610142	9.10E-6	0.090076451
164684	WBP2NL	WBP2 N-terminal like	18.099802	0.000997265	0.537803029
6863	TAC1	Tachykinin precursor 1	17.783615	1.76E-5	0.090076451
100302652	GPR75-ASB3	GPR75-ASB3 readthrough	17.145979	0.006635587	1
9956	HS3ST2	Heparan sulfate-glucosamine 3-sulfotransferase 2	16.512378	2.78E-5	0.090076451
3589	IL11	Interleukin 11	15.679315	2.30E-5	0.090076451
6781	STC1	Stanniocalcin 1	15.078708	2.78E-5	0.090076451
100533496	TVP23C-CDRT4	TVP23C-CDRT4 readthrough	14.787845	4.32E-5	0.094067798
5097	PCDH1	Protocadherin 1	14.36361	0.000160663	0.190391369
9132	KCNQ4	Potassium voltage-gated channel subfamily Q member 4	13.826998	0.003367649	0.943798303
9518	GDF15	Growth differentiation factor 15	13.606276	4.92E-5	0.095493868
9241	NOG	Noggin	13.556377	6.35E-5	0.096353188
1440	CSF3	Colony stimulating factor 3	12.750106	7.31E-5	0.101432911
11009	IL24	Interleukin 24	12.444253	0.000111668	0.144528797
645369	TMEM200C	Transmembrane protein 200C	11.927974	0.006295194	1
145741	C2CD4A	C2 calcium dependent domain containing 4A	11.541936	0.0003789	0.294238492
7056	THBD	Thrombomodulin	11.463245	0.000176524	0.190391369

(continued to the next page)

Table 1. (Continued) Top 40 up- and downregulated genes in fibroblasts after electrical stimulation

Gene_ID	Gene name	Gene description	Log2 FC	*p*-value	Adjusted *p*-value
26049	FAM169A	Family with sequence similarity 169 member A	10.87014	0.034780972	1
91156	IGFN1	Immunoglobulin like and fibronectin type III domain containing 1	10.439082	0.000589658	0.392610455
11211	FZD10	Frizzled class receptor 10	9.950769	0.00138752	0.615661579
3976	LIF	LIF interleukin 6 family cytokine	9.899971	0.000275404	0.243031891
390928	ACP7	Acid phosphatase 7, tartrate resistant (putative)	9.625839	0.001144039	0.584483548
3456	IFNB1	Interferon beta 1	9.554194	0.015150304	1
123722	FSD2	Fibronectin type III and SPRY domain containing 2	9.554194	0.015150304	1
2827	GPR3	G protein-coupled receptor 3	9.146792	0.000698429	0.437396554
50614	GALNT9	Polypeptide N-acetylgalactosaminyltransferase 9	8.749759	0.00222885	0.785690355
55607	PPP1R9A	Protein phosphatase 1 regulatory subunit 9A	8.591539	0.007116069	1
80201	HKDC1	Hexokinase domain containing 1	8.580175	0.001138873	0.584483548
5029	P2RY2	Purinergic receptor P2Y2	7.763279	0.006191067	1
388125	C2CD4B	C2 calcium dependent domain containing 4B	7.763279	0.006191067	1
114	ADCY8	Adenylate cyclase 8	7.37358	0.002042223	0.775305577
23025	UNC13A	Unc-13 homolog A	7.068924	0.002091116	0.775305577
3748	KCNC3	Potassium voltage-gated channel subfamily C member 3	6.879319	0.017459041	1
27237	ARHGEF16	Rho guanine nucleotide exchange factor 16	6.879319	0.017459041	1
9507	ADAMTS4	ADAM metallopeptidase with thrombospondin type 1 motif 4	6.839064	0.00190183	0.738442613
100507747	C13orf46	Chromosome 13 open reading frame 46	6.673782	0.009812054	1
5026	P2RX5	Purinergic receptor P2X 5	6.473408	0.009676606	1
6517	SLC2A4	Solute carrier family 2 member 4	6.445359	0.01348744	1

confirm the DEGs identified via RNA-seq. *Cavin-2*, which encodes Cavin-2, has been reported to modulate the morphology and function of the caveola of the plasma membrane, and *PIEZO2*, which encodes Piezo-type mechanosensitive ion channel component 2, is a mechanosensing cation channel that responds to diverse types of external forces[12,13]. qRT-PCR showed that electrical stimulation significantly downregulated *PIEZO2* and *CAVIN2* in dermal fibroblasts (**Fig. 3A**). Based on the results, we performed further experiments using siRNAs to confirm whether the inhibition of *PIEZO2* and *CAVIN2* affected type I procollagen production and MMP-1 expression in dermal fibroblasts. Our experimental results showed that siRNA transfection against *PIEZO2* significantly decreased type I collagen synthesis and increased MMP-1 expression in fibroblasts. As for *CAVIN2*, siRNA transfection significantly decreased type I collagen synthesis, while the change in MMP-1 expression was not significant.

DISCUSSION

In this study, we studied the effects of low-frequency and low-intensity electrical stimulation on the human dermal fibroblast and found that it effectively inhibited type I procollagen production and increased MMP-1 expression (**Fig. 4**). In addition, transcriptomic analyses revealed that electrical stimulation modulated the activity of various ion channels. Moreover, GO functional analysis suggested that the cellular membrane was affected by electrical stimulation. Finally, we validated the change in the expression of the mechanosensitive ion channel (*PIEZO2*) and membrane-bound protein organizing caveolae (*CAVIN2*) induced by electrical stimulation and found that electrical stimulation significantly reduced the expression of the two genes. Moreover, siRNA transfection revealed the role of these two genes in type I procollagen production and MMP-1 expression in human dermal fibroblasts. Our results demonstrate that electrical stimulation of human dermal fibroblasts plays a regulatory role in type I collagen production and MMP-1 expression by altering the membrane structure and function of human dermal fibroblasts.

For decades, researchers have tried to use electrical stimulation for influencing cell behaviors such as proliferation, differentiation, and migration[14]. Electrical stimulation has been reported to induce proliferation and differentiation of preosteoblasts, differentiation of neuronal stem cells into neuron, and morphological changes in myoblasts[14-17]. Based on multiple studies, the fundamental mechanisms of electrical stimulation on cells can be summarized into two hypotheses: electrical stimulation alters the transport of biomolecules and function of cellular membranes[18]. For skin, electrical stimulation has been used to facilitate the wound healing process by enhancing the proliferation and migration of skin cells[18-20]. However, contrary to wound healing where increased collagen synthesis is essential for optimal healing process, management of scar requires stimuli which suppress the collagen synthesis. Thus, it is necessary to explore novel electrical stimulation conditions that can suppress pathologically elevated collagen synthesis in the scar tissue.

Recently, electrical stimulation has been employed to suppress various cell functions for tumor treatment[6,21,22]. Using low-intensity (1–3 V/cm) and intermediate-frequency (100–300 kHz) AC, this

AD ANNALS of DERMATOLOGY

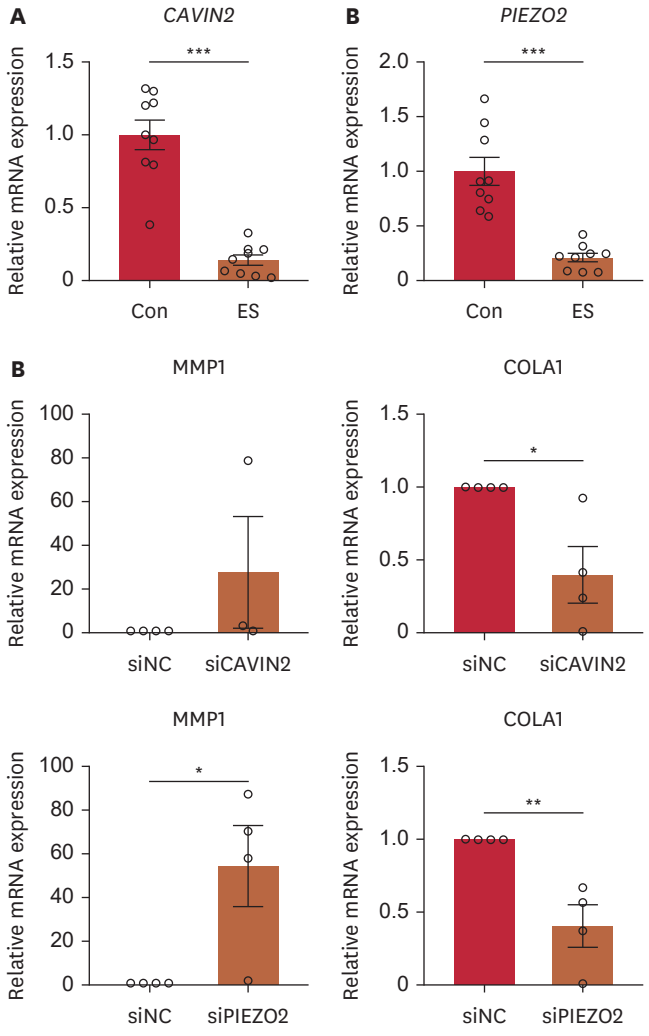

Fig. 3. Validation of differentially expressed genes using quantitative real time-polymerase chain reaction. (A) Quantitative reverse transcription polymerase chain reaction showed that electrical stimulation significantly downregulated *PIEZO2* and *CAVIN2* in dermal fibroblasts. (B) Inhibition of *PIEZO2* and *CAVIN2* via siRNA transfection significantly altered type I procollagen and matrix metalloproteinase-1 levels in dermal fibroblasts. *p<0.05, **p<0.01, ***p<0.001.

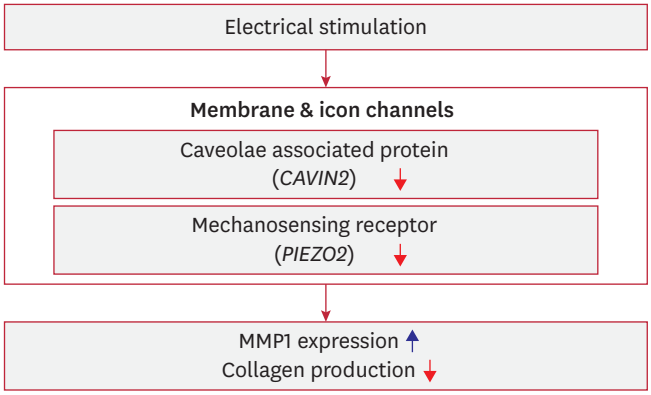

Fig. 4. Electrical stimulation of human dermal fibroblasts using low-frequency and low-intensity alternating current effectively modulated extracellular matrix homeostasis by altering cellular membrane structure and function.

electrical stimulation can inhibit tumor cell growth[22,23]. Studies on the fundamental mechanisms of its inhibitory effect on cancer cell function found that electrical stimulation increased cell membrane permeability, disrupted the cell membrane voltage, and inhibited cancer cell mitosis[21,22]. To modulate ECM production, we applied electrical stimulation using low-intensity (1 V/cm) and low-frequency (20 kHz) AC to primary human dermal fibroblast and found that low-intensity and low-frequency AC effectively inhibited type I procollagen synthesis in human dermal fibroblast without significantly affecting cell viability. Moreover, our transcriptomic analyses revealed that electrical stimulation altered membrane permeability by modulating the activity of ion channels and the structures of cellular membranes, including membrane rafts. The mechanisms of electrical stimulation of dermal fibroblasts are in line with the mechanism suggested to inhibit tumor cell function. Our findings indicate that ACs of low intensity and frequency in dermal fibroblasts regulate ECM production in the skin by altering plasma membrane structure and function.

Previously, the significance of tensile forces in the pathogenesis of hypertrophic scars and keloids were demonstrated[24,25]. This is corroborated by the observation that keloids on the anterior chest develop in a direction parallel to the tension lines[24-26]. In addition, the role of tension in scar formation has been substantiated through animal experimentation: African spiny mice with loose skin do not develop scars and undergo almost complete regeneration of the affected area[24,27]. Furthermore, tensile forces applied to the wound of animal model have been shown to result in an increase in α-smooth muscle actin expression, which is associated with the development of scar tissue[24,28]. In addition to tensile forces, recent studies have revealed that increased tissue stiffness can promote the overproduction of ECM by myofibroblasts, which leads to more stiff tissue, forming a vicious cycle that leads to hypertrophic scarring or keloid development[29,30]. To understand the reaction of fibroblasts to environmental forces, their mechanism of perceiving external mechanical forces has been studied. Fibroblasts in the skin sense mechanical stress through the Yes-associated protein 1/transcriptional coactivator with PDZ-binding motif signaling pathway, focal adhesion kinase-extracellular signal-regulated kinase pathway, or Piezo channels[24,25]. Among these mechanosensing receptors, one study revealed the elevated expression of Piezo1 in keloid hypertrophic scars, stimulation of fibroblast by Piezo1 activation, and the inhibition of Piezo1 with a chemical inhibitor protracted from hypertrophic scar formation in an animal model[31,32]. In this study, we found that electrical stimulation decreased Piezo2 expression in primary human fibroblasts. Although its role in hypertrophic scars and keloids has not been reported, Piezo2 has been suggested to play a critical role in the sensing of tissue stiffness in pulmonary

https://doi.org/10.5021/ad.25.001

tissue by fibroblasts, which promotes fibroblast differentiation into profibrotic myofibroblasts and induces ECM overproduction, leading to fibrosis of lung tissue[33]. In line with a previous study, our study suggests that electrical stimulation modulates ECM production by inhibiting Piezo2 expression in dermal fibroblasts.

Cavin-2, encoded by *CAVIN2*, is a calcium-independent phospholipid-binding protein that forms caveolae[34]. Previously, it was reported that the expression of Cavin-2 is associated with the number and morphology of caveolae and affects the stability of various receptors in caveolae[12,35]. The association of Cavin-2 in fibroblast with cardiac fibrosis has recently been reported[12]. Higuchi et al.[12] found that depletion of Cavin-2 decreased transforming growth factor (TGF)-β signaling, collagen synthesis of fibroblasts, and the number of α-smooth muscle actin-expressing myofibroblasts in mouse embryonic fibroblasts. They suggested that Cavin-2 plays a critical role in cardiac fibrosis by regulating TFG-β/Smad signaling. Consistent with previous study, we also found that fibroblasts stimulated with AC showed decreased *CAVIN2* expression. Thus, we can infer that the decrease in Cavin-2 expression by electrical stimulation induced changes in the cellular membrane, which modulated intracellular signaling for type I procollagen production and MMP-1 expression.

In conclusion, our study demonstrates that low-frequency and low-intensity electrical stimulation of human dermal fibroblasts effectively modulates ECM homeostasis by suppressing type I procollagen production and increasing MMP-1 expression. Our transcriptomic analysis suggests that low-frequency and low-intensity electrical stimulation induced significant alterations in the cellular membrane structure and function. These findings suggest a promising therapeutic approach for the management of keloid and hypertrophic scars by manipulating fibroblast function using external electrical stimulation.

ORCID iDs

Bo Mi Kang
https://orcid.org/0000-0003-2023-3971
Jung Min Ahn
https://orcid.org/0009-0005-6068-2415
Jieun Kim
https://orcid.org/0009-0009-6612-8414
Kyungho Paik
https://orcid.org/0000-0002-5706-2371
Bo Ri Kim
https://orcid.org/0000-0002-2223-1606
Dong Hun Lee
https://orcid.org/0000-0002-2925-3074
Sang Woong Youn
https://orcid.org/0000-0002-5602-3530
Keun-Yong Eom
https://orcid.org/0000-0003-3650-1133
Chong Won Choi
https://orcid.org/0000-0001-9994-8819

FUNDING SOURCE

This work was supported by the New Faculty Startup Fund from Seoul National University (grant number: 800-20210284) and the Seoul National University Bundang Hospital Research Fund (grant number: 02-2024-0016).

CONFLICTS OF INTEREST

The authors have nothing to disclose.

DATA SHARING STATEMENT

The data that support the findings of this study are available from the corresponding author upon reasonable request.

SUPPLEMENTARY MATERIAL

Supplementary Fig. 1

Viability of primary human dermal fibroblasts measured using Annexin V and PI staining after electrical stimulation.

REFERENCES

1. Cheah YJ, Buyong MR, Mohd Yunus MH. Wound healing with electrical stimulation technologies: a review. Polymers (Basel) 2021;13:3790. PUBMED | CROSSREF
2. Nuccitelli R. A role for endogenous electric fields in wound healing. Curr Top Dev Biol 2003;58:1-26. PUBMED | CROSSREF
3. Melotto G, Tunprasert T, Forss JR. The effects of electrical stimulation on diabetic ulcers of foot and lower limb: a systematic review. Int Wound J 2022;19:1911-1933. PUBMED | CROSSREF
4. Feedar JA, Kloth LC, Gentzkow GD. Chronic dermal ulcer healing enhanced with monophasic pulsed electrical stimulation. Phys Ther 1991;71:639-649. PUBMED | CROSSREF
5. Borges D, Pires R, Ferreira J, Dias-Neto M. The effect of wound electrical stimulation in venous leg ulcer healing-a systematic review. J Vasc Surg Venous Lymphat Disord 2023;11:1070-1079.e1. PUBMED | CROSSREF
6. Tanzhu G, Chen L, Xiao G, Shi W, Peng H, Chen D, et al. The schemes, mechanisms and molecular pathway changes of Tumor Treating Fields (TTFields) alone or in combination with radiotherapy and chemotherapy. Cell Death Dis 2022;8:416. PUBMED | CROSSREF
7. Jenkins EPW, Finch A, Gerigk M, Triantis IF, Watts C, Malliaras GG. Electrotherapies for glioblastoma. Adv Sci (Weinh) 2021;8:e2100978. PUBMED | CROSSREF
8. Chun Q, ZhiYong W, Fei S, XiQiao W. Dynamic biological changes in fibroblasts during hypertrophic scar formation and regression. Int Wound J 2016;13:257-262. PUBMED | CROSSREF
9. Macarak EJ, Wermuth PJ, Rosenbloom J, Uitto J. Keloid disorder: Fibroblast differentiation and gene expression profile in fibrotic skin diseases. Exp Dermatol 2021;30:132-145. PUBMED | CROSSREF
10. Perry D, Colthurst J, Giddings P, McGrouther DA, Morris J, Bayat A. Treatment of symptomatic abnormal skin scars with electrical stimulation. J Wound Care 2010;19:447-453. PUBMED | CROSSREF
11. Hernández-Bule ML, Toledano-Macías E, Pérez-González LA, Martínez-Pascual MA, Fernández-Guarino M. Anti-fibrotic effects of

RF electric currents. Int J Mol Sci 2023;24:10986. PUBMED | CROSSREF

12. Higuchi Y, Ogata T, Nakanishi N, Nishi M, Tsuji Y, Tomita S, et al. Cavin-2 promotes fibroblast-to-myofibroblast trans-differentiation and aggravates cardiac fibrosis. ESC Heart Fail 2024;11:167-178. PUBMED | CROSSREF
13. Zheng M, Borkar NA, Yao Y, Ye X, Vogel ER, Pabelick CM, et al. Mechanosensitive channels in lung disease. Front Physiol 2023;14:1302631. PUBMED | CROSSREF
14. Chen C, Bai X, Ding Y, Lee IS. Electrical stimulation as a novel tool for regulating cell behavior in tissue engineering. Biomater Res 2019;23:25. PUBMED | CROSSREF
15. Kumar A, Nune KC, Misra R. Understanding the response of pulsed electric field on osteoblast functions in three-dimensional mesh structures. J Biomater Appl 2016;31:594-605. PUBMED | CROSSREF
16. Li N, Zhang Q, Gao S, Song Q, Huang R, Wang L, et al. Three-dimensional graphene foam as a biocompatible and conductive scaffold for neural stem cells. Sci Rep 2013;3:1604. PUBMED | CROSSREF
17. Jaatinen L, Young E, Hyttinen J, Vörös J, Zambelli T, Demkó L. Quantifying the effect of electric current on cell adhesion studied by single-cell force spectroscopy. Biointerphases 2016;11:011004. PUBMED | CROSSREF
18. Zhao S, Mehta AS, Zhao M. Biomedical applications of electrical stimulation. Cell Mol Life Sci 2020;77:2681-2699. PUBMED | CROSSREF
19. Thakral G, Lafontaine J, Najafi B, Talal TK, Kim P, Lavery LA. Electrical stimulation to accelerate wound healing. Diabet Foot Ankle 2013;4:22081. PUBMED | CROSSREF
20. Zhao M, Song B, Pu J, Wada T, Reid B, Tai G, et al. Electrical signals control wound healing through phosphatidylinositol-3-OH kinase-gamma and PTEN. Nature 2006;442:457-460. PUBMED | CROSSREF
21. Karanam NK, Story MD. An overview of potential novel mechanisms of action underlying Tumor Treating Fields-induced cancer cell death and their clinical implications. Int J Radiat Biol 2021;97:1044-1054. PUBMED | CROSSREF
22. Li X, Liu K, Xing L, Rubinsky B. A review of tumor treating fields (TTFields): advancements in clinical applications and mechanistic insights. Radiol Oncol 2023;57:279-291. PUBMED | CROSSREF
23. Kirson ED, Dbalý V, Tovarys F, Vymazal J, Soustiel JF, Itzhaki A, et al. Alternating electric fields arrest cell proliferation in animal tumor models and human brain tumors. Proc Natl Acad Sci U S A 2007;104:10152-10157. PUBMED | CROSSREF
24. Harn HI, Ogawa R, Hsu CK, Hughes MW, Tang MJ, Chuong CM. The tension biology of wound healing. Exp Dermatol 2019;28:464-471. PUBMED | CROSSREF
25. Tsai CH, Ogawa R. Keloid research: current status and future directions. Scars Burn Heal 2019;5:2059513119868659. PUBMED | CROSSREF
26. Akaishi S, Akimoto M, Ogawa R, Hyakusoku H. The relationship between keloid growth pattern and stretching tension: visual analysis using the finite element method. Ann Plast Surg 2008;60:445-451. PUBMED | CROSSREF
27. Seifert AW, Kiama SG, Seifert MG, Goheen JR, Palmer TM, Maden M. Skin shedding and tissue regeneration in African spiny mice (Acomys). Nature 2012;489:561-565. PUBMED | CROSSREF
28. Squier CA. The effect of stretching on formation of myofibroblasts in mouse skin. Cell Tissue Res 1981;220:325-335. PUBMED | CROSSREF
29. Hinz B. Tissue stiffness, latent TGF-beta1 activation, and mechanical signal transduction: implications for the pathogenesis and treatment of fibrosis. Curr Rheumatol Rep 2009;11:120-126. PUBMED | CROSSREF
30. Handorf AM, Zhou Y, Halanski MA, Li WJ. Tissue stiffness dictates development, homeostasis, and disease progression. Organogenesis 2015;11:1-15. PUBMED | CROSSREF
31. Jiang Z, Chen Z, Xu Y, Li H, Li Y, Peng L, et al. Low-frequency ultrasound sensitive piezo1 channels regulate keloid-related characteristics of fibroblasts. Adv Sci (Weinh) 2024;11:e2305489. PUBMED | CROSSREF
32. He J, Fang B, Shan S, Xie Y, Wang C, Zhang Y, et al. Mechanical stretch promotes hypertrophic scar formation through mechanically activated cation channel Piezo1. Cell Death Dis 2021;12:226. PUBMED | CROSSREF
33. Freeberg MAT, Camus SV, Thatcher TH, Sime PJ. Piezo2 is an important mechano-receptor in pulmonary fibrosis. Am J Respir Crit Care Med 2024;209:A5184. CROSSREF
34. Gustincich S, Vatta P, Goruppi S, Wolf M, Saccone S, Della Valle G, et al. The human serum deprivation response gene (SDPR) maps to 2q32-q33 and codes for a phosphatidylserine-binding protein. Genomics 1999;57:120-129. PUBMED | CROSSREF
35. Boopathy GTK, Kulkarni M, Ho SY, Boey A, Chua EWM, Barathi VA, et al. Cavin-2 regulates the activity and stability of endothelial nitric-oxide synthase (eNOS) in angiogenesis. J Biol Chem 2017;292:17760-17776. PUBMED | CROSSREF